Article

Tracking the impact of climate factors on vegetation dynamics across the Alashan Plateau semi desert ecoregion

SeyedOmid Reza Shobairi[1], **Samira Hemmati Roudbari**[2], **Qirghizbek Ayombekov**[1], **Hadis Sadeghi**[3], **BehnamAsghari Beirami**[4], **MehranAlizadeh Pirbasti**[5]

[1]Xinjiang Institute of Ecology and Geography, Chinese Academy of Sciences, Urumqi 830011, China

[2]Department of Soil Science, Faculty of Agriculture, University of Zanjan, Iran

[3]Climate Research Institute, Atmospheric Science and Meteorological Research Center, Iran

[4]Department of Photogrammetry and Remote Sensing, K. N. Toosi University of Technology, Tehran, Iran

[5]Department of Remote Sensing, Hekmat Institute of Higher Education, Qom, Iran

E-mail: Omidshobeyri214@gmail.com, omid@ms.xjb.ac.cn

Received 4 October 2023; *Accepted 10 November 2023*; *Published online 20 November 2023*; *Published 1 June 2024*

(cc) BY

Abstract

Several studies have demonstrated global climate change, which has happened worldwide; it significantly impacts terrestrial ecosystems. Studying vegetation phenology can provide insight into the impact of climate changes on ecosystems. Alashan Plateau Semi-Desert is located between the Tibetan Plateau and the Gobi Desert and has an arid continental climate. This area consists of highlands, and the sensitivity of natural vegetation to temperature and climate change is very high. This study aims to identify climate trends in forest cover indices using weather (meteorological) data from 1982 to 2019 across the Alashan Plateau Semi-Desert. Based on this, 13 variables that affect climate change were selected, and the possible effect of climate factors on vegetation indices was predicted using MATLAB. The results showed that over the past 38 years, three forest cover indices, LAI, FAPAR, and NDVI, decreased by about 6-10, 6-7, and 19-20 percent correspondingly, and it can be assumed that this decline is due to climate change. In general, it can be said that climate changeshave adverse effects in hot and dry regions and highlands. With the current climate change trends, such as increasing temperature and decreasing rainfall, reducing the dynamics of vegetation indices in these areas can be seen dramatically.

Keywords NDVI; LAI; FAPAR; climate drivers; ecoregions; Alashan Plateau.

Computational Ecology and Software
ISSN 2220-721X
URL: http://www.iaees.org/publications/journals/ces/online-version.asp
RSS: http://www.iaees.org/publications/journals/ces/rss.xml
E-mail: ces@iaees.org
Editor-in-Chief: WenJun Zhang
Publisher: International Academy of Ecology and Environmental Sciences

1 Introduction

Currently, vegetation change measures regional or global environmental conditions (Deng et al., 2019*)*. Due to climate change and the increased frequency and intensity of extreme events, terrestrial ecosystems have been adversely affected, desertification and land degradation have been accelerated in many regions, and food

security has been negatively affected as a result (Fahadet al., 2021; Huang et al., 2020). Increasing atmospheric CO_2 levels, land cover changes, and climatic changes affect vegetation differently, so the impact of climate changes on vegetation has gathered increasing attention in recent years (Kong et al., 2018; Fahad et al., 2021b, 2021a, 2021d). It has been shown that changes in plant phenology are related to climate change. Therefore a change in plant phenology can be regarded as a sign that the climate is changing and that species have adapted to the new environment (Parmesan et al., 2003; Visser et al., 2005; Zhou et al., 2022). Therefore, understanding how plant phenology shifts in response to changes in climate can assist us in understanding the dynamics of vegetation during future climate change (Tao et al., 2017).

Phenology derived from time series of remote sensing indices has proven to be a reliable method for estimating the large-scale growth stage of vegetation (Frankenberg et al., 2018; Piao et al., 2019). Piao et al. (2020) examined recent advances in plant phenology and their interaction with climate change. Recent research has demonstrated that the rapid expansion of ground-based and remote sensing-based phenology data acquisition has led to significant advancements in plant phenology research. According to many global studies, the use of normalized difference vegetation index (NDVI), leaf area index (LAI), and the fraction of absorbed photosynthetically active radiation (FAPAR) has been proposed to evaluate the consistency between vegetation and terrestrial essential climate variables retrieved from Earth observation on a global scale. NDVI index is used to assess the ecological impact of global warming, ecological change, agricultural status, land change, and desertification. In addition to estimating vegetation in forests and non-forests, NDVI is widely used in analyzing how climate change is affecting forest and non-forest vegetation productivity (Ols et al., 2019; Chu et al., 2019; Zhao et al., 2020; Li et al., 2021; Zhe et al., 2021; Jiang et al., 2021; Liu et al., 2021b; Liu et al., 2021c). LAI, defined as half of the leaf surface area in a canopy in a given area and used to describe canopy structure, is a measure of photosynthetic activity in vegetation and plant health (Baret et al., 1989). LAI is a crucial variable regulating the biosphere and climate interaction. It regulates the surface energy balance of the surface, the hydrological cycle, the carbon budget, and the boundary layer meteorology. LAI is used to demonstrate terrestrial ecosystems' complex and dynamic processes and to analyze responses to environmental conditions. LAI also makes it possible to predict the terrestrial carbon flux and its effect on atmospheric CO_2 concentration. An accurate representation of seasonal LAI in models is essential to simulate terrestrial ecosystem dynamics and their interactions with the environment in climatic simulations (Jeong et al., 2020; Piao et al., 2020). The remote sensing-based LAI products were also used to estimate land surface phenology (Verger et al., 2016; Song et al., 2020). Using satellite-derived LAI products, Verger et al. (2016) found that LAI is more suitable than NDVI or EVI for estimating land surface phenology in dense vegetation areas. FAPAR represents the fraction of active photosynthetic radiation absorbed by green/living elements that determine the photosynthetic status of vegetation and is used to monitor vegetation status and ecosystem productivity and to simulate a wide range of responses. Ecological studies are applied to climate change and atmospheric chemical composition, including changes in the distribution of plant communities (Chen et al., 2019).

Various climatic factors influence the Vegetation phenology, growth, development, distribution, decline, and seasonal vegetation changes, such as temperature, precipitation, insolation, humidity, etc. Furthermore, the climate is defined as a seasonal period of solar radiation, temperature, and precipitation that primarily determines terrestrial vegetation types, including broadleaved forests, grasslands, and biogeochemical properties of the earth's surface (such as CO_2 flux and carbon storage in biomass and soil) (Tao et al., 2017; Cleland et al., 2007).

Several studies have examined the effects of changes in climatic variables such as air temperature and precipitation on vegetation indicators (Gao et al., 2022; Shang et al., 2022; Sun et al., 2021; Gao et al., 2021).

Climate factors such as temperature and precipitation regulate vegetation growth (Wang et al., 2016; Braswell et al., 1997; Guo et al., 2021). By calibrating and computing time series from satellite-derived NDVI during 1982-2012, In the Northern Hemisphere, the spatial variability and temporal trends of vegetation phenology were surveyed by Wang et al. (2016). Furthermore, the authors examined the response of vegetation in different ecological zones to climate change.Based on their findings, it was concluded that temperature plays a crucial role in determining vegetation phenology, and the response of vegetation phenology to temperature varied across different eco-zones. Climate change will affect vegetation growth periods and the composition and morphology of vegetation itself (Liu et al., 2015; Sun et al., 2015; Deng et al., 2017; De et al., 2015). It has been reported that the driving factors of climate on vegetation have gradually shifted to precipitation and temperature (Sun et al., 2021; Gao et al., 2022). Thus, precipitation and temperature, the two most direct and significant climate factors, are chosen for studies of vegetation change in response to climate change (Gao et al., 2021). Shang et al. (2022) found that precipitation and temperature were the most important factors affecting NDVI changes in northwest China.

The relationship between vegetation phenology, vegetation growth, development of their types and distribution, and even anomalies and destruction by climate drivers is crucial in global change research. It indicates dynamic feedback of terrestrial ecosystems to climate changes. Therefore, monitoring the above-complicated process is very important for future climate change. Recently, the standard method of collecting plant phenology has been based on field techniques (such as cluster sampling) to observe individual organisms regularly and record changes that occur visually, such as budburst, flowering, foliation, or defoliation. However, remote sensing technologies have recently assisted us in predicting climate change trends over space and time.

Alashan Plateau semi-desert includes low mountains and deserts, except for the southwest of the Gobi desert. This area benefits from the rainfall of the Tibetan Plateau, but it is only enough to water the vegetation of arid and semi-arid areas. According to the KöppenBWk index, this region is considered one of the cold and dry regions. It has the characteristics of dry lands, i.e., low rainfall, high evaporation, and transpiration, and temperature fluctuations during the day and night. Annual rainfall in the Alashan region is lower than 150 mm.

Therefore, the wildlife of this region and the plant community are compatible with the conditions of this ecosystem and have many strategies for their development, formation, and survival. Due to the fragility of this ecosystem and the particular importance of this region for North China and the Mongolian plateau, and as far it allows us to study tracking climate-vegetation interaction and phenological changes and their drivers across ecoregions in the Alashan Plateau semi-desert over the past 38 years by coding on existing platforms and extraction and calculation of remotely sensed datasets. We predict the possible impact of climate factors on vegetation indexes using MATLAB.

2 Material and Methods

2.1 Study area

The Alashan Plateau semi-desert ecoregion is located on the southwestern margin of the Gobi Desert, where a short period of summer precipitation is sufficient to support a sparse plant community. The terrain in the area consists of basins and ranges with altitudes ranging from 1000 to 2500 m (3300 to 8200 feet).The region is straddled by the China-Mongolian border, with the Tibetan Plateau to the south and the more arid regions of the Gobi to the north and east. A desert basin and low mountains encompass the ecoregion, bordered on the west by the Lop Desert, on the south by the Tibetan Plateau and the Qilian Mountains, and on the north and southeast by the Gobi extension of the Altai Mountains. Despite being in the rain shadow of the Tibetan Plateau, parts of the Gobi desert still receive sufficient precipitation to sustain semi-arid desert plant

communities (Fig. 1). There is a cool arid climate in this ecoregion (KöppenBWk). In this climate, precipitation is typically below the potential evapotranspiration rate in arid climates. Several months average below 0°C (32°F). Annual precipitation on the Alashan Plateau is under 150 mm (6 in/year).

Alashan Plateau plant communities employ a variety of strategies to survive and form. Areas of sand characterize this ecoregion, and bare rock, low-lying areas dominated by salt-tolerant plants (halophytes) and plants adapted to low precipitation levels (xerophytes). The presence of shrubs such as Haloxylonammodendron and Reaumuriasoongorica, which are semi-perennials, contributes to the stability of the soil and attracts other plant species. There are semi-desert communities of artemisia, Zygophyllum, and calligonummongolicum in areas with more moisture. A small area of grassland is supported by runoff from the Qilian Mountains, and a river forest of desert poplar (Populuseuphratica) and Tamarix species is supported by the Yellow River, which runs along the eastern edge of the area. Table 1 shows the area and its percentage.

Table 1 Area and percentage of Alashan area of China.

Object ID	Ecoregion (Eco-name)	Biome	Protected area	Area_km2	Percent_Area
1	Alashan Plateau semi-desert	Deserts & Xeric Shrublands	Nature Could Reach Half Protected	457798.5484	4.889396004

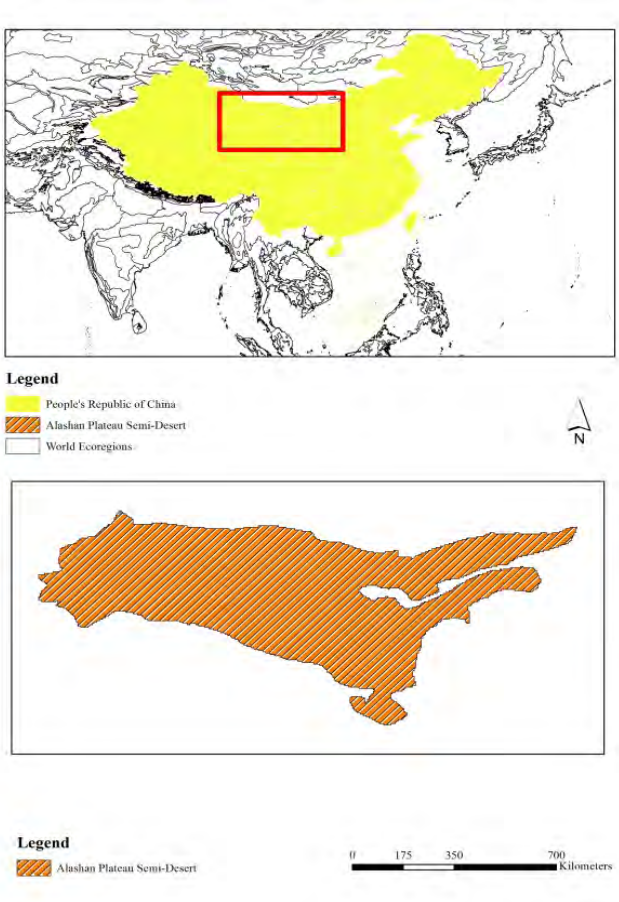

Fig. 1 Alashan Plateau semi-desert across the china ecoregions.

2.2 Datasets

Table 2 provides a summary of the data sources used for this study. Since the NDVI data from GIMMS cover a long period and wide coverage, they have proven useful in studying regional and global vegetation change (Zhu et al., 2020). This study used the advanced high-resolution radiometer (NOAA-AVHRR) series of data collected from the National Oceanic and atmospheric administration to produce the GIMMS NDVI data set. This data set was collected from 1980 to 2013 using the Google Earth engine due to its high volume of data, and other data were gathered from NOAA and NASA disks for long-term data (Shen et al., 2021). Also, NOAA AVHRR LAI products were used because LAI has a better and more accurate simulation of vegetation density. This dataset contains gridded Fraction of Absorbed Photosynthetically Active Radiation (FAPAR) and daily Leaf Area Index (LAI) derived from the NOAA Climate Data Record (CDR) of Advanced Very High-Resolution Radiometer (AVHRR) Surface Reflectance. Data was collected by eight NOAA polar-orbiting satellites from 1981 to 2019: NOAA-7, -9, -11, -14, -16, -17, -18, and -19. It is projected on a global grid of 0.05 degrees × 0.05 degrees. The NASA Goddard Space Flight Center (GSFC) and the University of Maryland (UMD) produced this dataset as part of the Land Surface CDR project (Wang et al., 2021). The data related to the climate factor were extracted from TRMM data/precipitation/3 hour and monthly or from the Parsiann ccs precipitation website or GLDAF climate data.

Table 2 Major data sources.

Satellite / Model	Product Name	Data Name	Unit	Spatial Resolution	Temporal Resolution	Time Extent	Coverage
NOAA (AVHRR)	Climate Data Record (CDR)	NDVI LAI FAPAR	nan	5 km	Monthly	24/6/1981	Global
ERA5	ECMWF atmospheric reanalysis	Air Temperature	k	25 km	Monthly	1/1/1979	Global
		Total Precipitation	m				
		Surface Pressure	pa				
		Soil Moisture	$m^3 m^{-3}$				
FLDAS	FEWS NET	Downward longwave radiation flux	$w m^{-2}$	10 km	Monthly	1/1/1982	Global
		Soil Heat Flux	$w m^{-2}$				
		Sensible heat net flux	$w m^{-2}$				
		Latent Heat Flux	$w m^{-2}$				
		Snow Depth	m				
		Snow cover fraction	nan				
		Snowfall Rate	$kg m^{-2} s^{-1}$				
		Snow Water Equivalent	$kg m^{-2}$				
TERRA Climate	University of IDAHO	Wind Speed	m/s	4 km	Monthly	1/1/1958	Global
		Palmer Drought Index	nan				

Data were collected By the Google Earth Engine platform from 1982 to 2019. GEE is a cloud computing platform that combines time series archives of earth observation data, tools, and algorithms. The list of the applieddata is as follows:

- NDVI/NOAA daily - 1982 to 2019 - 5 km spatial resolution - Global scale
- NDVI/NOAA Twice a month - 1982 to 2019 - 5 km spatial resolution - Global scale
- LAI & FAPAR/NOAA daily - 1982 to 2019 - 5 km spatial resolution - Global scale
- EVI/NOAA - 2000 to 2020 - Global scale and also below datasets;
- Surface Pressure
- Palmer Drought Index
- Snow Water Equivalent
- Soil Moisture
- Downward Shortwave Radiation
- Wind Speed
- Downward Longwave Radiation
- Net Longwave Radiation Flux
- Soil Heat Flux
- Sensible Heat Flux
- Latent Heat Flux
- Snowfall Rate
- Snow Water Equivalent
- Net Shortwave Radiation Flux

The image collections were cross-tabulated with the ecoregions with a mean filter reducer. Each observation was aggregated for each ecoregion for the average NDVI, rainfall, temperature, and other values.

2.3 Technical route

A flowchart depicting the methods used to determine the phenological feedback from NDVI, LAI, and FAPAR time series concerning climate factors is shown in Fig. 2. Time series of NDVI, LAI, and FAPAR were calculated monthly from 1982 to 2019, first for the ecoregions of China and then for the semi-desert ecoregion of Alashan. Temperature time series and precipitation changes for about forty years have been obtained. We were making a model for soil moisture, soil temperature, drought, wind speed, light, heat, snow depth, topography, and other factors related to plant phenology (growth and development). Climate change is causing these changes. Visual patterns also were calculated to understand the changes by QGIS further. Also, our dependent variables in this research were plant indices NDVI, FAPAR, and LAI, which were influenced by our independent variables, i.e., climatic and environmental factors. The relationship between dependent and independent variables was calculated using Excel and artificial intelligence techniques in the MATLAB platform. Furthermore, our predictions came true that climatic and environmental drivers influence vegetation dynamics, and in fragile environments, this effect is doubled.

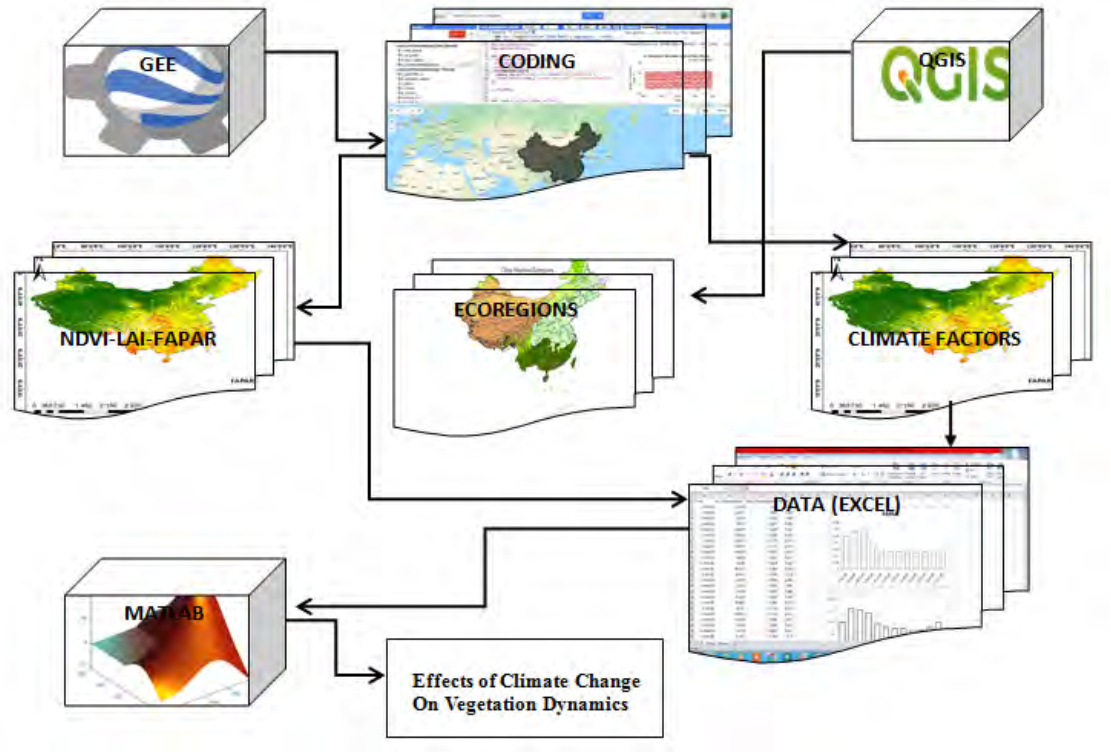

Fig. 2 Main flowchart of procedures.

3 Result and discussion

3.1 Change in the percentage decrease in LAI, FAPAR, and NDVI from 1982 to 2019

For 38 years, from 1982 to 2019, three forest cover indices, LAI, FAPAR, and NDVI, were measured sequentially, as well as weather data of 13 characteristics. Three forest cover indices are positively correlated: coefficients were 0.75 between LAI and FAPAR, 0.51 between NDVI and FAPAR, and 0.16 between LAI and NDVI.

Our study aims to identify climate trends in forest cover indices using weather (meteorological) data. We produced the study of the obtained experimental data according to a two-stage procedure used earlier in analyzing the distribution of larch NPP in Northern Eurasia.

Stage 1. In the first stage, we attempted to trace the *LAI, FAPAR,* and *NDVI* concerning the main external weather characteristics measured every month for 38 years, which are as the following:

T – air temperature,
P - total precipitation,
SP - surface pressure,
SHF - soil heat flux,
SH - sensible heat flux,
LH - latent heat flux,
SM - soil moisture content,

DLR - downward longwave radiation,
DSR - downward shortwave radiation,
SW - snow water equivalent,
SD - snow depth,
PD - Palmer drought index,
WS - the wind speed.

We analyzed the multiple linear relationships of each forest cover index with the entire set of weather characteristics correlated with each other. The total set of weather-independent variables explained the variability of *LAI*, *FAPAR*, and *NDVI* by 75, 47, and 22 %, respectively. It turned out that of all the independent variables in the three equations, the most significant was the soil heat flux (*SHF*). In the equations for *LAI*, *FAPAR*, and *NDVI*, the Student's criterion for the independent variable *SHF* was equal to 4.5, 2.9, and 6.1, respectively. Most of the other weather variables in the multiple regression equations were not statistically significant at the probability level of 0.95. The dependencies *LAI*, *FAPAR*, and *NDVI* on *SHF* are calculated as follows:

$LAI = 0.1268+0.0042\ SHF$; adj $R^2 = 0.633$; SE = 0.03 (1)
$FAPAR = 0.0914+0.00081\ SHF$; adj $R^2 = 0.469$; SE = 0.008 (2)
$NDVI = 0.0786+0.00015\ SHF$; adj $R^2 = 0.06$; SE = 0.01 (3)

When the *NDVI* index was approximated using the full set of independent variables, the student's criterion was the highest for the variable *SHF* (6.1>1.96). Most of the other variables were statistically unreliable at the probability level of 0.95. However, when the index was approximated using this single reliable independent variable, the coefficient of determination dropped sharply from 0.22 to 0.03. However, the independent variable *SHF* is statistically significant at the probability level of 0.999 (t = 4.1>2.0).

Our goal is to identify the most significant independent variable associated with *LAI*, *FAPAR*, and *NDVI*, calculate corresponding equations, and track how these relationships change with calendar years in the range from 1982 to 2019.

Therefore, we introduce the factor of calendar years encoded by the block of dummy into equations (1)-(3) variables (De Jong et al., 2011):

LAI, *FAPAR* and *NDVI* $= a+b\ SHF +j\ \Sigma Xi$ (4)

where $\Sigma Xi = cX1+dX2+eX3+…..nX37$. The calendar years 1982, 1983, 1984, … 2019 are coded by dummy variables as *X*0, *X*1, *X*2, *X*3+…..*X*37. After calculating equation (4), we prepare the matrixes of initial data to identify the dynamics of *LAI*, *FAPAR*, and *NDVI* dependence on *SHF* from 1982 to 2019 (Table 3).

Stage 2. As we move from 1982 to 2019, the ratio of the consecutive intercept of dummy variables of equation (4) to the intercept of the initial equation calculated for the initial year 1982 decreases monotonically. The description of the mentioned dependence represents the second stage of the two-stage procedure of our analysis. We described the percentage decrease in the value of the intercept of equation (4) from 1982 to 2019, shown in the following table:

LAI = 3.3890 -0.2624 X; R^2 = 0.274; SE = 4.45 (5)
$FAPAR$ = 0.7191-0.1750 X; R^2 = 0.505; SE = 1.90 (6)
$NDVI$ = 4.9573-0.6479 X; R^2 = 0.341; SE = 9.76 (7)

For regression coefficients -0.2624, -0.1750, and -0.6479, the t-statistics are 3.8, 6.1, and 4.5, which exceeds the standard value of 1.96 at the probability level of 0.999. The geometric interpretation of equations (5)-(7) against the background of actual data is given in Fig. 3.

According to Fig. 3, we can see that in the range of calendar years from 1982 to 2019, there is a monotonous decrease in the change in the percentage of *LAI*, *FAPAR*, and *NDVI*, provided that the level of *SHF* remains unchanged. It does not correlate with the mentioned temporal range and has a mean value of 0.128.

Thus, over the past 38 years, three forest cover indices, *LAI*, *FAPAR*, and *NDVI*, under conditions where the main external weather characteristics *SHF* remains unchanged, are decreased by about 6-10, 6-7, and 19-20 % correspondingly. It can be assumed that this decline is due to climate change.

3.2 Spatial and temporal patterns of changes in NDVI, LAI, and FAPAR

The Alashan Plateau Semi-Desert is located between the Tibetan Plateau and the Gobi Desert, which has an arid continental climate, primarily highland areas, and vegetation susceptible to temperature changes and climate change (Gao et al., 2022; Li et al., 2021; Li et al., 2019). Climate change affects vegetation due to changes in temperature, rainfall, solar radiation, nutrient cycles, microbial activity, and physiological activity within plants. Rainfall changes may alter moisture regimes, salinity, acidity, soil erosion, and other chemical and physical factors. All these factors affect vegetation growth (Chen et al., 2017; Zhu et al., 2020; Wang et al., 2021). The results of this study show that the vegetation of the Alashan Plateau Semi-Desert area has generally decreased from 1982 to 2019, except in parts of the northeast and small areas of the southern strip. According to the visual patterns related to Fig. 4, it can be said that there is a trend of increasing NDVI, LAI, and FAPAR values in the southern and northeastern parts of the Alashan region.In other places, such as the central, northern, and western parts of the Alashan region, we see a decrease in vegetation indicators, which shows these parts' fragility. There are two aspects to the process of vegetation activity reacting to climate change, which can explain the heterogeneity in the values of vegetation indices in some regions. The first characteristic is the nonlinearity of the effect of climate factors on vegetation.For example, warming the environment can increase vegetation activity before reaching the optimum temperature for photosynthesis. This trend has been observed in this study in the southern and northeastern regions of the Alashan Plateau (Fig. 5(a)). Air temperature gain) and in other studies in the Tibetan Plateau.Second, hydrological and thermal factors interact to determine vegetation activity. For example, increasing evapotranspiration may increase the propensity for drought. This trend was observed in most areas of the Alashan Plateau. However, this may decrease with increasing rainfall. In this study, increased vegetation activity in the southern regions of the Alashan Plateau is observed with increasing temperature and rainfall (Lotsch et al., 2005). Guo et al. (2021) reported different patterns of vegetation change in Inner Mongolia in their study on vegetation dynamics. Forests and desert meadows had partially improved vegetation, but conventional grasslands in the central part of the country had partially degraded. This result is consistent with that of this study, which shows that vegetation has increased in some areas of the northeast and in a small amount of the southern strip, and in other areas, it has decreased significantly.

Table 3 Preparation of a matrix of initial data to identify the dynamics of *LAI*, *FAPAR*, and *NDVI* dependence on *SHF* for the period from 1982 to 2019.

Calendar year	The number of the calendar year (*X*)	Independent variable	*LAI*		*FAPAR*		*NDVI*	
			The regression coefficient	*Y* *	The regression coefficient	*Y* *	The regression coefficient	*Y* *
1982	0	Intercept	0.13032	0	0.09419	0	0.08559	0
-	-	*SHF*	0.00413	-	0.00081	-	0.00009	-
1983	1	X_1	0.00474	3.63	-0.00034	-0.36	-0.00371	-4.34
1984	2	X_2	0.00416	3.19	0.00067	0.71	-0.00073	-0.86
1985	3	X_3	-0.00005	-0.04	-0.00068	-0.72	-0.00149	-1.74
1986	4	X_4	0.00011	0.08	-0.00183	-1.95	-0.00396	-4.63
1987	5	X_5	0.00462	3.55	-0.00096	-1.02	-0.00332	-3.88
1988	6	X_6	-0.00048	-0.37	-0.00258	-2.74	-0.01205	-14.07
1989	7	X_7	0.00168	1.29	0.00081	0.86	-0.01924	-22.48
1990	8	X_8	-0.00363	-2.78	-0.00245	-2.60	-0.00136	-1.59
1991	9	X_9	-0.00126	-0.96	-0.00029	-0.31	-0.00145	-1.69
1992	10	X_{10}	0.00046	0.35	-0.00129	-1.37	-0.00573	-6.69
1993	11	X_{11}	0.00225	1.73	-0.00031	-0.33	-0.00522	-6.10
1994	12	X_{12}	0.00299	2.30	-0.00014	-0.14	0.01325	15.49
1995	13	X_{13}	-0.00028	-0.22	-0.00102	-1.08	0.00789	9.22
1996	14	X_{14}	0.00067	0.51	-0.00124	-1.31	0.00620	7.24
1997	15	X_{15}	0.00543	4.17	0.00034	0.36	0.01331	15.55
1998	16	X_{16}	0.00257	1.97	0.00058	0.62	0.00791	9.24
1999	17	X_{17}	0.00960	7.36	0.00249	2.65	0.00865	10.10
2000	18	X_{18}	0.00456	3.50	-0.00026	-0.27	0.00645	7.54
2001	19	X_{19}	-0.00160	-1.22	-0.00198	-2.10	0.00048	0.57
2002	20	X_{20}	0.00119	0.92	-0.00235	-2.50	-0.00150	-1.75
2003	21	X_{21}	-0.00140	-1.08	-0.00262	-2.78	-0.01085	-12.67
2004	22	X_{22}	-0.00178	-1.36	-0.00325	-3.45	-0.00846	-9.89
2005	23	X_{23}	-0.00206	-1.58	-0.00307	-3.26	-0.00971	-11.35
2006	24	X_{24}	-0.00529	-4.06	-0.00742	-7.88	-0.01638	-19.14
2007	25	X_{25}	-0.00343	-2.63	-0.00241	-2.56	-0.00136	-1.59
2008	26	X_{26}	-0.01341	-10.29	-0.00654	-6.94	-0.01136	-13.27
2009	27	X_{27}	-0.00716	-5.49	-0.00489	-5.19	-0.01179	-13.78
2010	28	X_{28}	-0.00550	-4.22	-0.00719	-7.63	-0.02347	-27.42
2011	29	X_{29}	-0.01777	-13.63	-0.00563	-5.97	-0.01654	-19.33
2012	30	X_{30}	-0.01450	-11.13	-0.00461	-4.89	-0.01535	-17.94
2013	31	X_{31}	-0.00663	-5.09	-0.00529	-5.62	-0.01332	-15.56
2014	32	X_{32}	-0.00765	-5.87	-0.00649	-6.89	-0.01745	-20.39
2015	33	X_{33}	-0.01168	-8.96	-0.00650	-6.90	-0.01992	-23.27
2016	34	X_{34}	-0.00333	-2.55	-0.00502	-5.33	-0.01931	-22.56
2017	35	X_{35}	0.00098	0.75	-0.00346	-3.67	-0.01771	-20.69
2018	36	X_{36}	0.00243	1.86	-0.00508	-5.39	-0.01864	-21.78
2019	37	X_{37}	-0.00857	-6.58	-0.00271	-2.88	-0.02247	-26.25

* Y is the ratio of the consecutive intercept of dummy variables of equations (4) to the intercept of the initial equation calculated for the original year 1982, %.

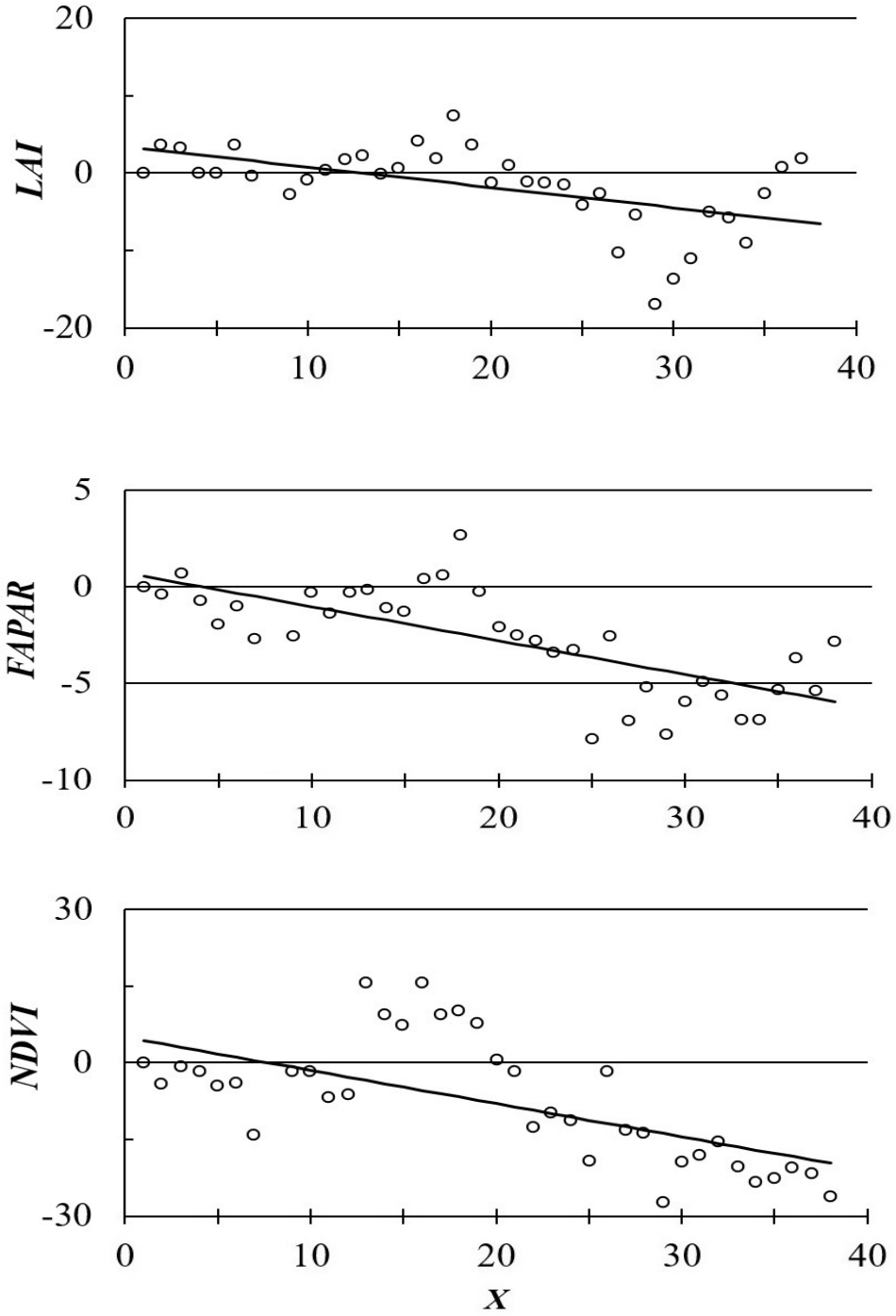

Fig. 3 Declining indices of *LAI*, *FAPAR*, and *NDVI* (in %%) over 38 years (*X* is the ordinal number of the calendar year from 1982 to 2019).

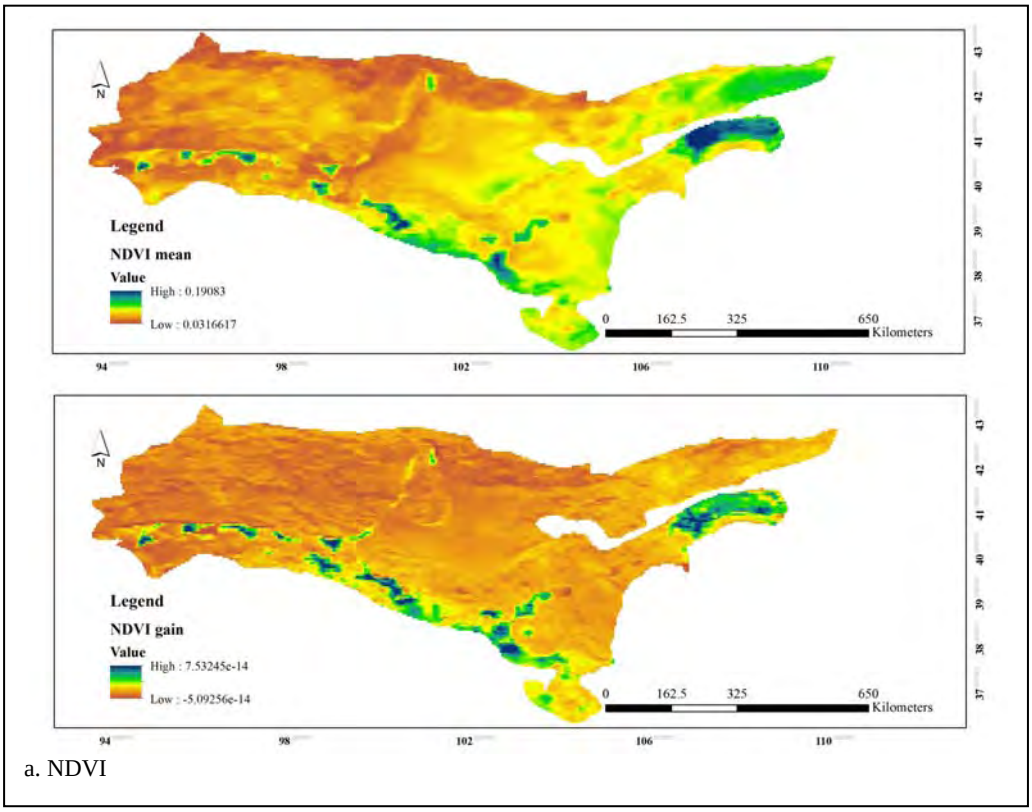
Legend
NDVI mean
Value
High : 0.19083
Low : 0.0316617
0 162.5 325 650
Kilometers
94 98 102 106 110
37 38 39 40 41 42 43
Legend
NDVI gain
Value
High : 7.53245e-14
Low : -5.09256e-14
0 162.5 325 650
Kilometers
94 98 102 106 110
37 38 39 40 41 42 43

a. NDVI

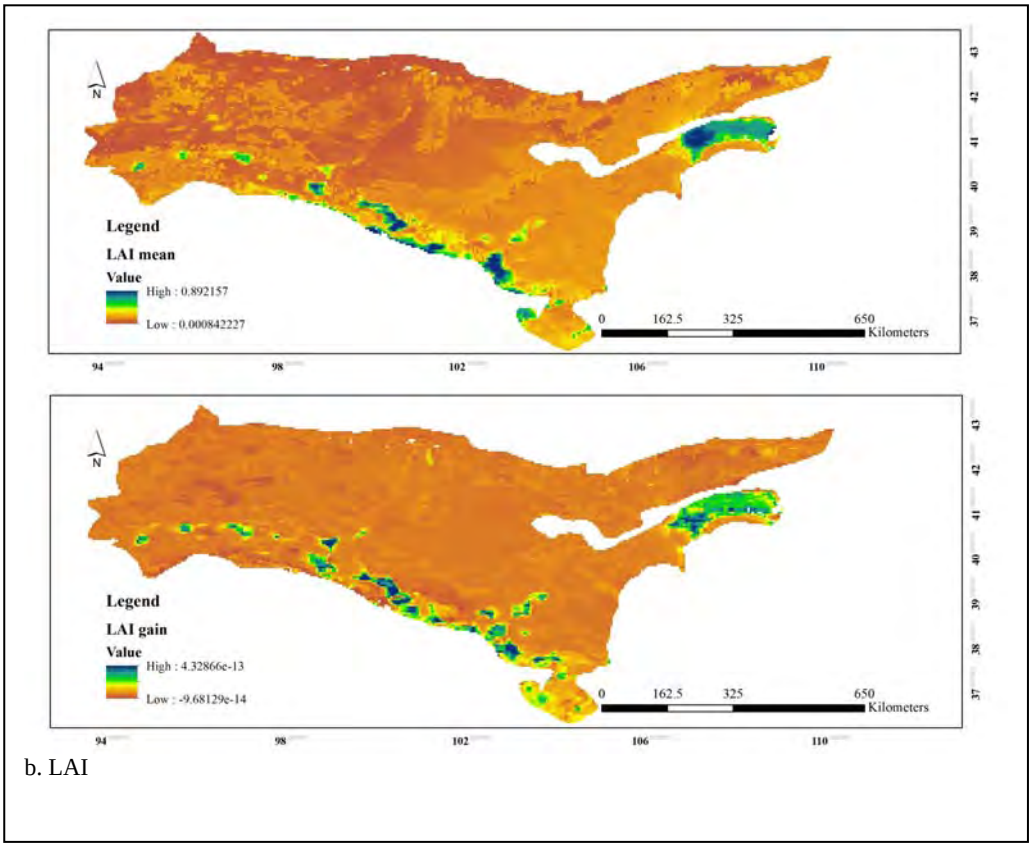
Legend
LAI mean
Value
High : 0.892157
Low : 0.000842227
0 162.5 325 650
Kilometers
94 98 102 106 110
37 38 39 40 41 42 43
Legend
LAI gain
Value
High : 4.32866e-13
Low : -9.68129e-14
0 162.5 325 650
Kilometers
94 98 102 106 110
37 38 39 40 41 42 43

b. LAI

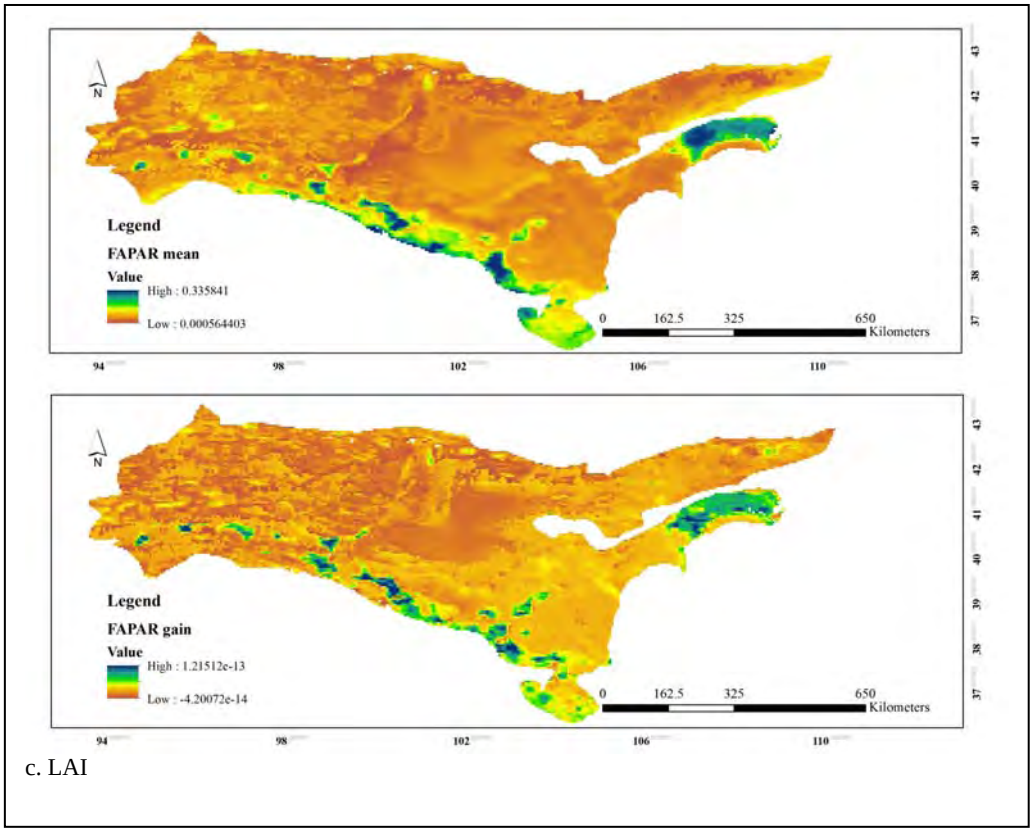

c. LAI

Fig. 4 The visual patterns of the three plant indices (NDVI: a, LAI: b, FAPAR: c).

3.3 The effects of climatic variables in NDVI, LAI, and FAPAR

Climate variability and climate change significantly impact plant phenology, an essential bioindicator of climate change (Shen et al., 2015; Li et al., 2016; Ramos et al., 2017; Zhu et al., 2017; Prăvălie et al., 2018). Over the last few decades, the global climate has undergone several unprecedented changes, and global warming has proven to be indisputable (Kong et al. 2020).Phenology is also affected by other environmental factors, such as photoperiod, precipitation, atmospheric CO_2, and nitrogen concentrations (Jeonj et al., 2011; Peñuelas et al., 2004; Linderholm et al., 2006; Nord et al., 2009; Xie et al., 2015). Consequently, in recent years, increasing attention has been paid to the effects of global climate change on vegetation growth (De Jong et al., 2011; Kong et al., 2018, 2020; Guo et al., 2021).

The study of the 38-year trend of changes in climate parameters in the Alashan Plateau semi-desert region shows that general warming with an overall increase in evapotranspiration with a relative decrease in rainfall and an increase in drought in most areas of the Alashan Plateau semi-desert has happened. As regards these parameters are generally recognized as key climatic stimuli for vegetation change, and also that their dynamics represent significant changes in climatic conditions over decades, the decrease in vegetation indices of NDVI, LAI, and FAPAR in the Alashan Plateau Semi-Desert area can be attributed to factors influencing climate change.

Vegetation growth is influenced by precipitation and temperature (Braswell et al., 1997; Guo et al., 2021). Climate change will affect vegetation growth periods, composition, and morphology (Sun et al., 2015; Deng et al., 2017). It has been reported that the driving factors of climate on vegetation have gradually shifted to precipitation and temperature (Sun et al., 2021; Gao et al., 2022). Moreover, precipitation and temperature are usually selected as significant factors for studying the impact of climate factors on vegetation change (Gao et

al., 2021). A study by Shang et al. (2022) showed that The NDVI changes in northwest China were primarily influenced by precipitation and temperature. In northwest China, Wang et al. (2021) found that precipitation had a much more significant effect on vegetation growth in arid areas than on grassland. The results of temperature changes during this research show that the air temperature has increased throughout the Alashan region, and this increase has occurred significantly in the southern regions (Fig. 5a). The results of previous studies have shown that rising temperatures have reduced vegetation indices in some areas, such as western and northern China. This decrease can be due to the decrease in the growing season due to rising temperatures, especially in arid and semi-arid regions in northern China, the decrease in rainfall, and the existence of the Tibetan Plateau, which is fragile due to high ecosystems and vegetation growth in this area is severely affected by water and air, was explained. Numerous studies have attributed the decline in NDVI since the 1990s or early 2000s, especially in arid and semi-arid regions of northern China, to drought stresses enhanced by warmer weather and less rainfall (Lotsch et al., 2005; Xiong et al., 2019; Sun et al., 2021). Also, based on the average precipitation map (Fig. 5b) in the Alashan region, it can be seen that the amount of precipitation is significantly more in the southern regions than in other places. The amount of precipitation has decreased over the past 40 years in the south-central, northeastern, and northwestern regions (Fig. 5b). Therefore, it can be said that a general trend of warming and drying has occurred in the Alashan region, with an increase in the average temperature and a decrease in precipitation.

According to the Palmer Drought Index gain (Fig. 5l), the Palmer Index's value has increased in the northern regions, especially in the northeast and northwest. As observed, the amount of rainfall in these areas has decreased significantly. Furthermore, the decrease in Palmer index in the mentioned areas and, consequently, the increase in drying trend can be explained, and it can be stated that humidity conditions were the primary controlling factor affecting the growth of vegetation in the area, which is consistent with their findings (Li et al., 2019). According to previous studies, the highest prevalence of drought is found in the eastern half of Inner Mongolia, the western part of the northwest, the northeast half of China, and small parts of the northeast.

Human activities have a significant impact on vegetation changes in addition to climate change (Chen et al., 2019; Shi et al., 2021). As we know, grassland is a kind of widespread vegetation that occupies the Alashan Plateau Semi-Desert area. In this region, in addition to climatic effects such as reduced rainfall, increased drought, and increased temperature, the human population and the number of livestock, which are the primary forms of human activity in this region, accelerate the destruction of pastures and grasslands. Also, agricultural production, overgrazing of livestock, increase in population, rapidly developing economy, and urbanization have occurred continuously in the past decades (Chen et al., 2017). All these factors in reducing Vegetation indices play a role. Therefore, it can be said that while climate change in this region is severe and the process of warming and drying is significantly intensified, human factors also effectively reduce the development of vegetation dynamics. Other environmental and climatic visual patterns can also be understood for the studied time series (Fig. 5).

Human activities have a significant impact on vegetation changes in addition to climate change (Chen et al., 2019; Shi et al., 2021). As we know, grassland is a kind of widespread vegetation that occupies the Alashan Plateau Semi-Desert area. In this region, in addition to climatic effects such as reduced rainfall, increased drought, and increased temperature, the human population and the number of livestock, which are the primary forms of human activity in this region, accelerate the destruction of pastures and grasslands. Also, agricultural production, overgrazing of livestock, increase in population, rapidly developing economy, and urbanization have occurred continuously in the past decades (Chen et al., 2017). All these factors in reducing Vegetation indices play a role. Therefore, it can be said that while climate change in this region is severe and the process of warming and drying is significantly intensified, human factors also effectively reduce the development of

vegetation dynamics. Other environmental and climatic visual patterns can also be understood for the studied time series (Fig. 5).

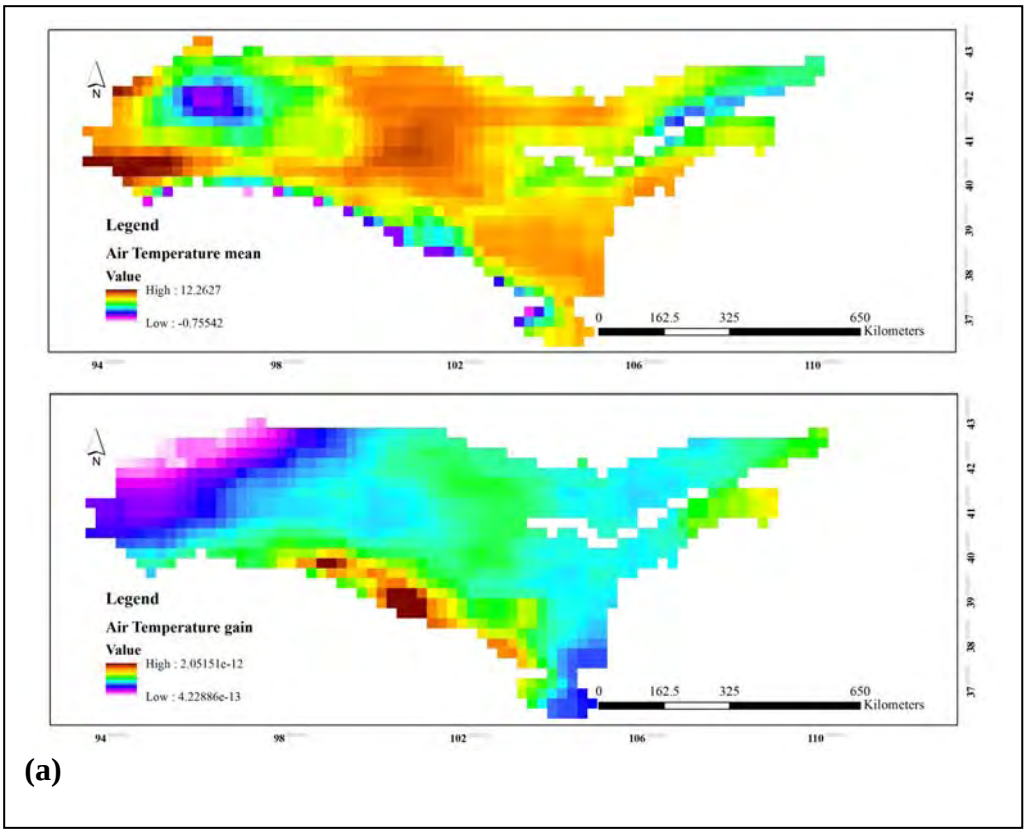

(a)

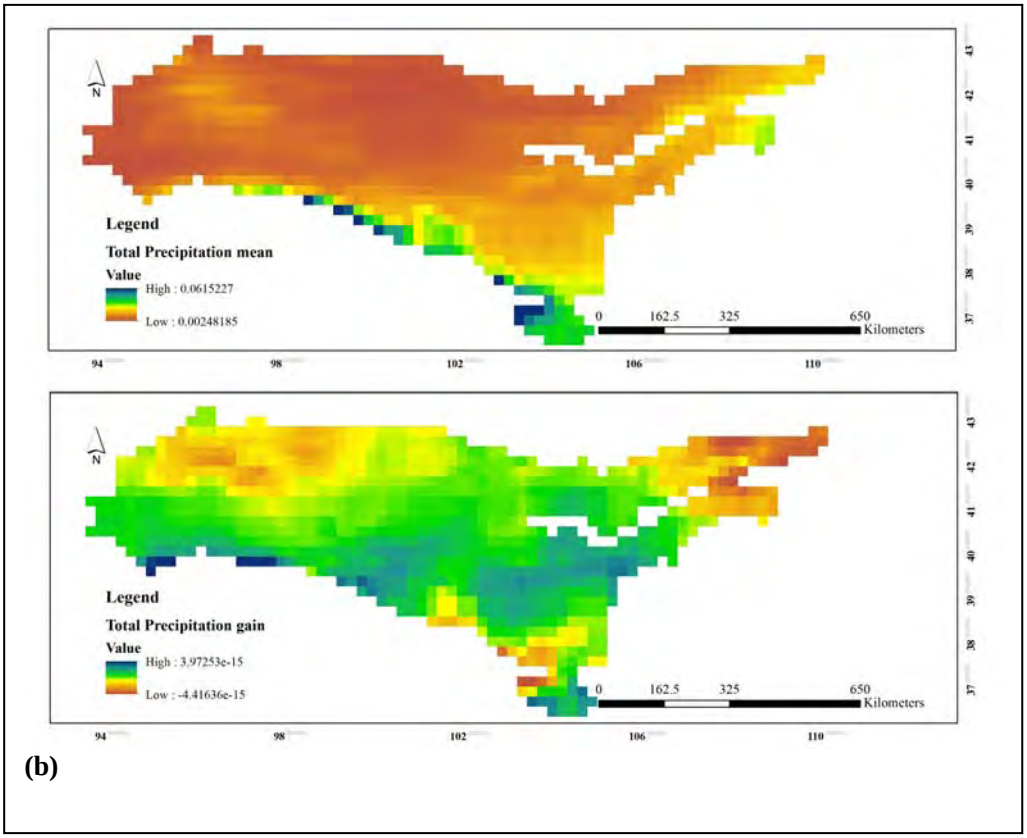

(b)

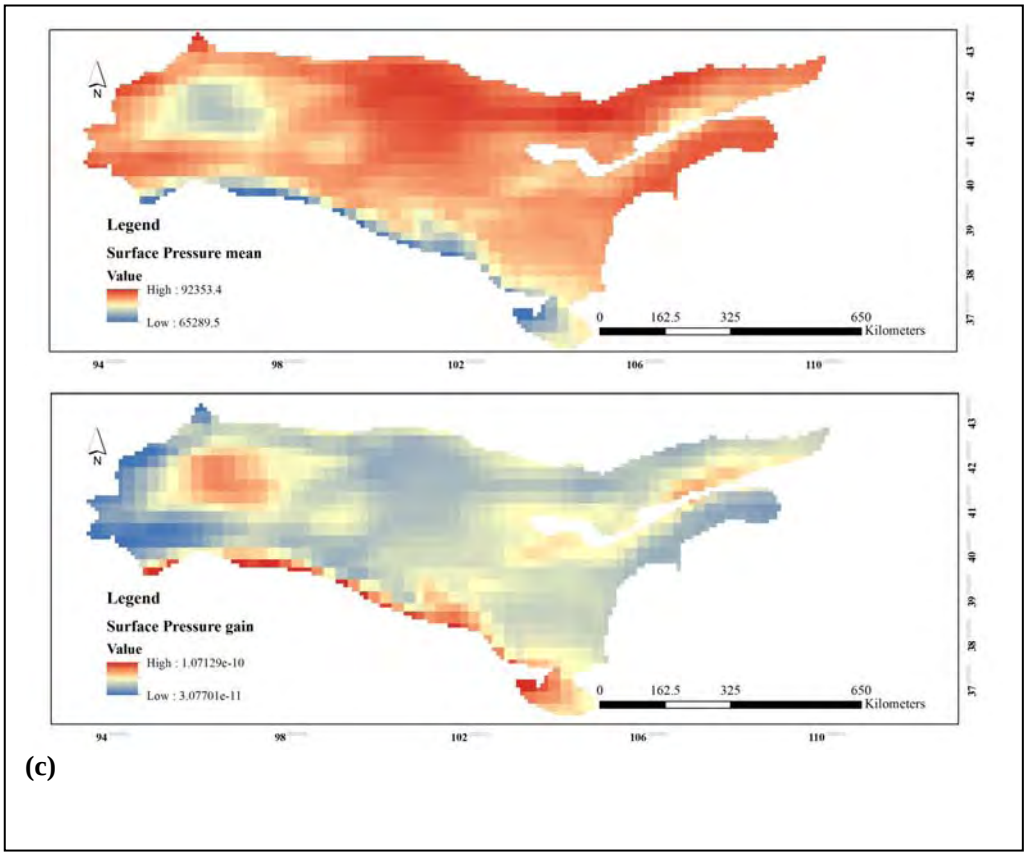
N
Legend
Surface Pressure mean
Value
High : 92353.4
Low : 65289.5
0 162.5 325 650
Kilometers
94 98 102 106 110
37 38 39 40 41 42 43
N
Legend
Surface Pressure gain
Value
High : 1.07129e-10
Low : 3.07701e-11
0 162.5 325 650
Kilometers
94 98 102 106 110
37 38 39 40 41 42 43

(c)

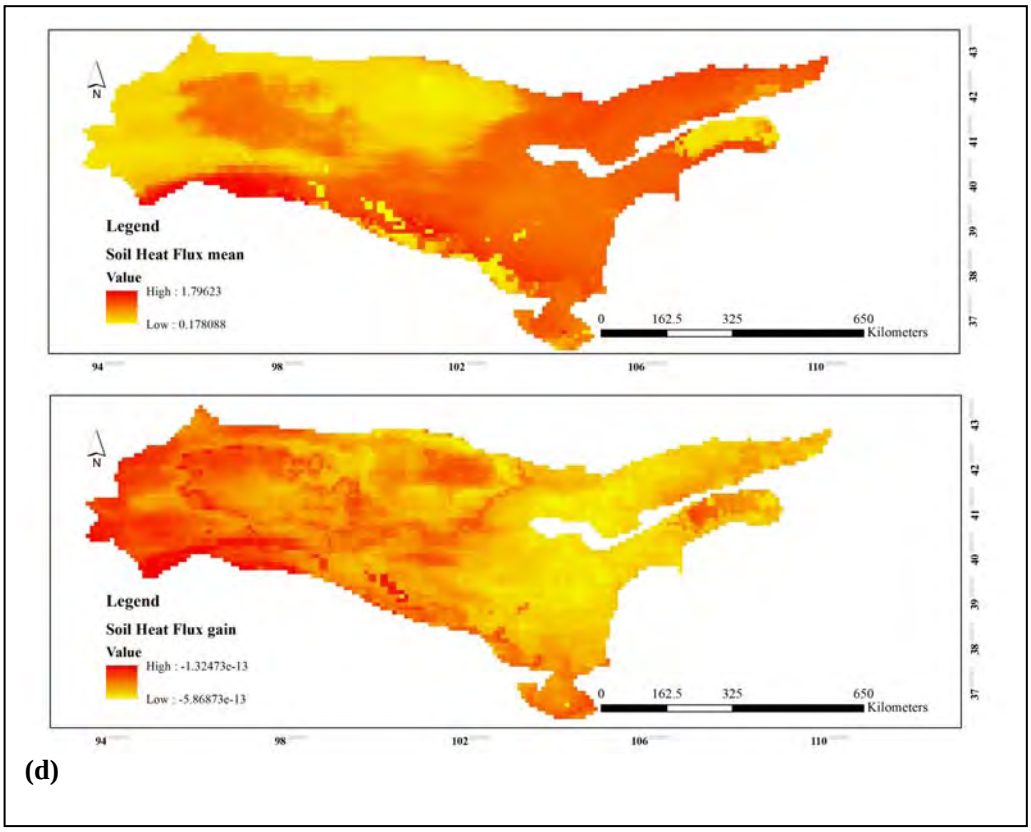
N
Legend
Soil Heat Flux mean
Value
High : 1.79623
Low : 0.178088
0 162.5 325 650
Kilometers
94 98 102 106 110
37 38 39 40 41 42 43
N
Legend
Soil Heat Flux gain
Value
High : -1.32473e-13
Low : -5.86873e-13
0 162.5 325 650
Kilometers
94 98 102 106 110
37 38 39 40 41 42 43

(d)

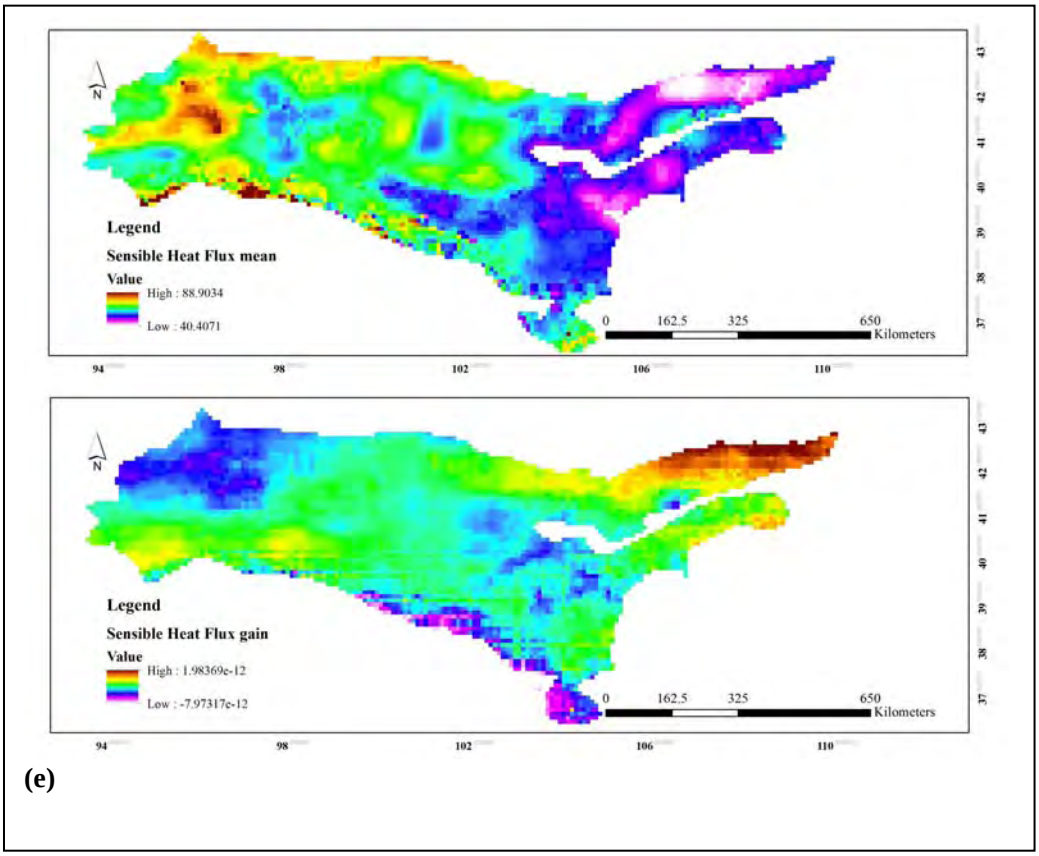
N
Legend
Sensible Heat Flux mean
Value
High : 88.9034
Low : 40.4071
0 162.5 325 650
Kilometers
94 98 102 106 110
37 38 39 40 41 42 43
N
Legend
Sensible Heat Flux gain
Value
High : 1.98369e-12
Low : -7.97317e-12
0 162.5 325 650
Kilometers
94 98 102 106 110
37 38 39 40 41 42 43

(e)

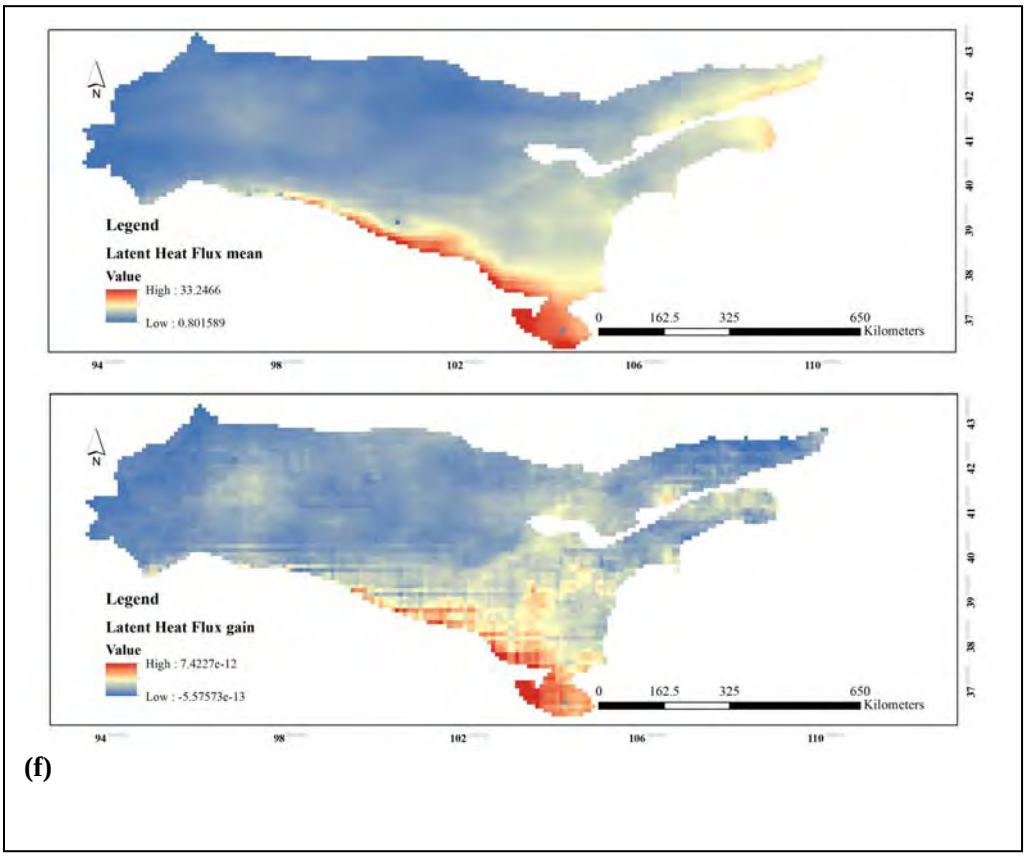
N
Legend
Latent Heat Flux mean
Value
High : 33.2466
Low : 0.801589
0 162.5 325 650
Kilometers
94 98 102 106 110
37 38 39 40 41 42 43
N
Legend
Latent Heat Flux gain
Value
High : 7.4227e-12
Low : -5.57573e-13
0 162.5 325 650
Kilometers
94 98 102 106 110
37 38 39 40 41 42 43

(f)

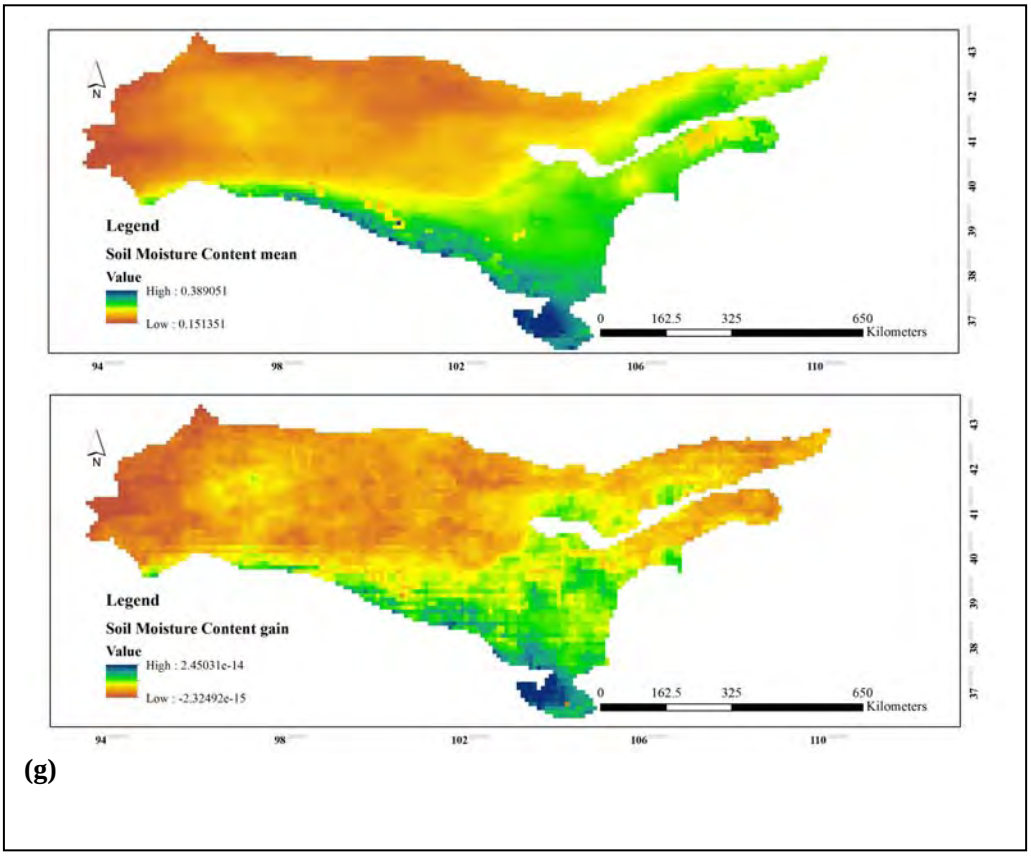
N
Legend
Soil Moisture Content mean
Value
High : 0.389051
Low : 0.151351
0 162.5 325 650
Kilometers
94 98 102 106 110
37 38 39 40 41 42 43
N
Legend
Soil Moisture Content gain
Value
High : 2.45031e-14
Low : -2.32492e-15
0 162.5 325 650
Kilometers
94 98 102 106 110
37 38 39 40 41 42 43

(g)

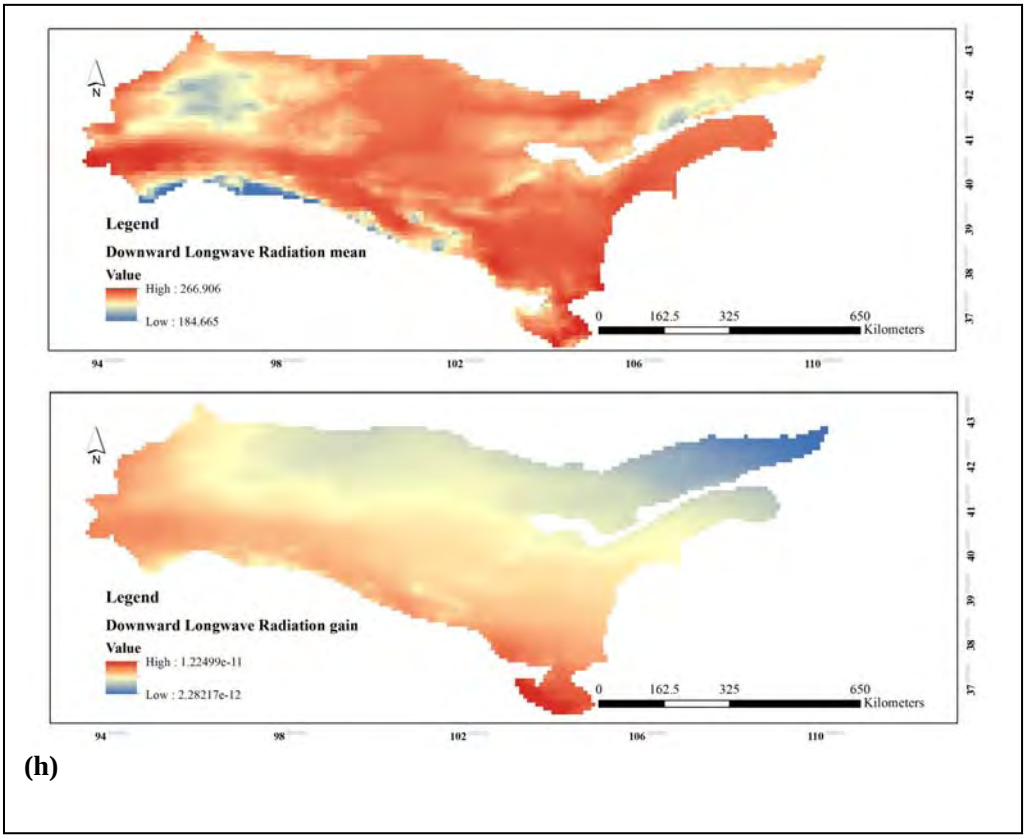
N
Legend
Downward Longwave Radiation mean
Value
High : 266.906
Low : 184.665
0 162.5 325 650
Kilometers
94 98 102 106 110
37 38 39 40 41 42 43
N
Legend
Downward Longwave Radiation gain
Value
High : 1.22499e-11
Low : 2.28217e-12
0 162.5 325 650
Kilometers
94 98 102 106 110
37 38 39 40 41 42 43

(h)

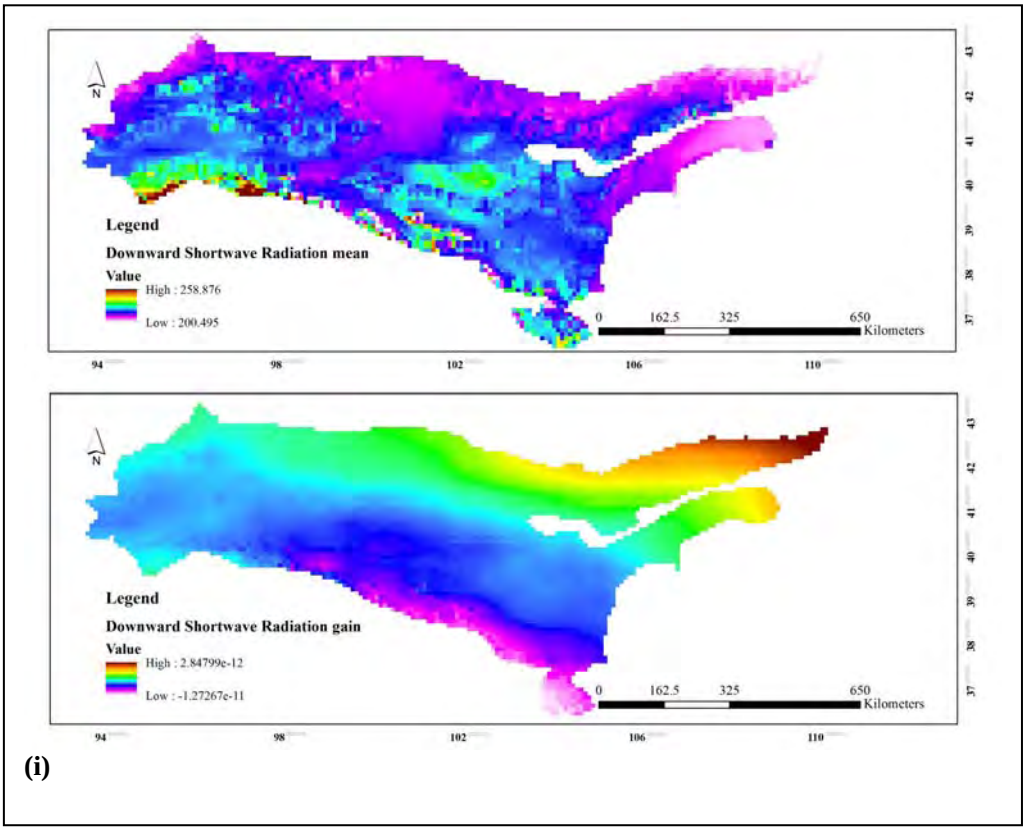
N
Legend
Downward Shortwave Radiation mean
Value
High : 258.876
Low : 200.495
0 162.5 325 650
Kilometers
94 98 102 106 110
37 38 39 40 41 42 43
N
Legend
Downward Shortwave Radiation gain
Value
High : 2.84799e-12
Low : -1.27267e-11
0 162.5 325 650
Kilometers
94 98 102 106 110
37 38 39 40 41 42 43

(i)

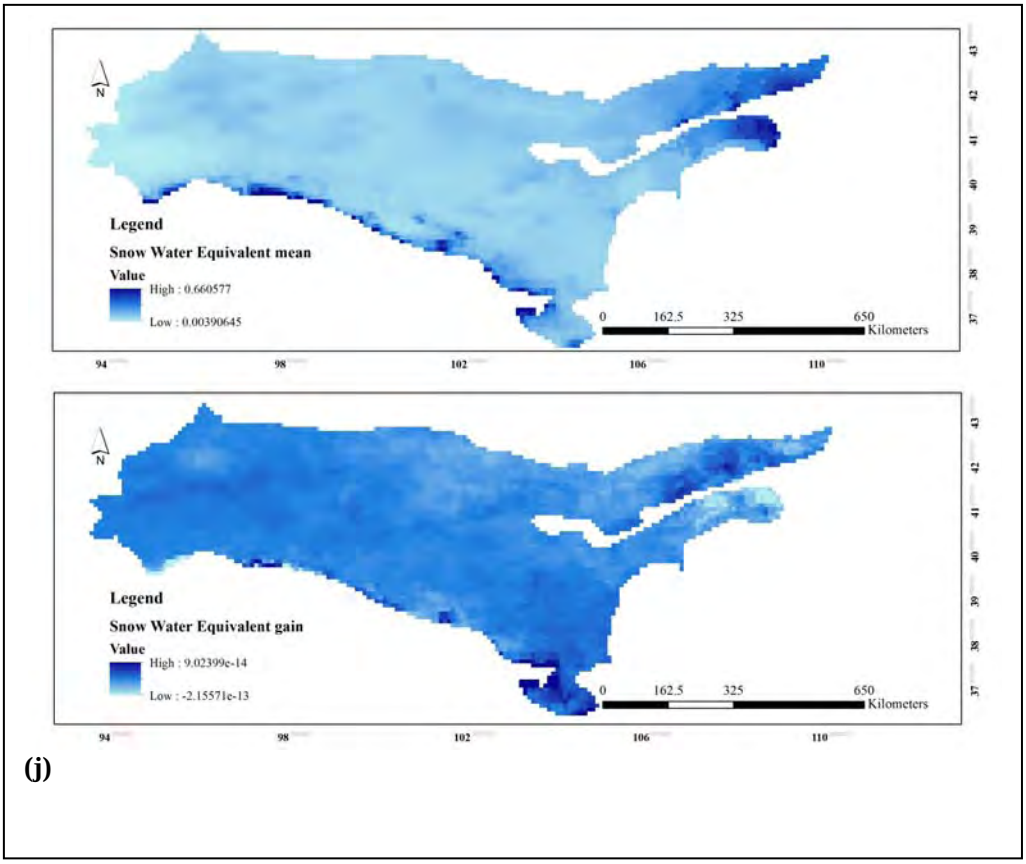
N
Legend
Snow Water Equivalent mean
Value
High : 0.660577
Low : 0.00390645
0 162.5 325 650
Kilometers
94 98 102 106 110
37 38 39 40 41 42 43
N
Legend
Snow Water Equivalent gain
Value
High : 9.02399e-14
Low : -2.15571e-13
0 162.5 325 650
Kilometers
94 98 102 106 110
37 38 39 40 41 42 43

(j)

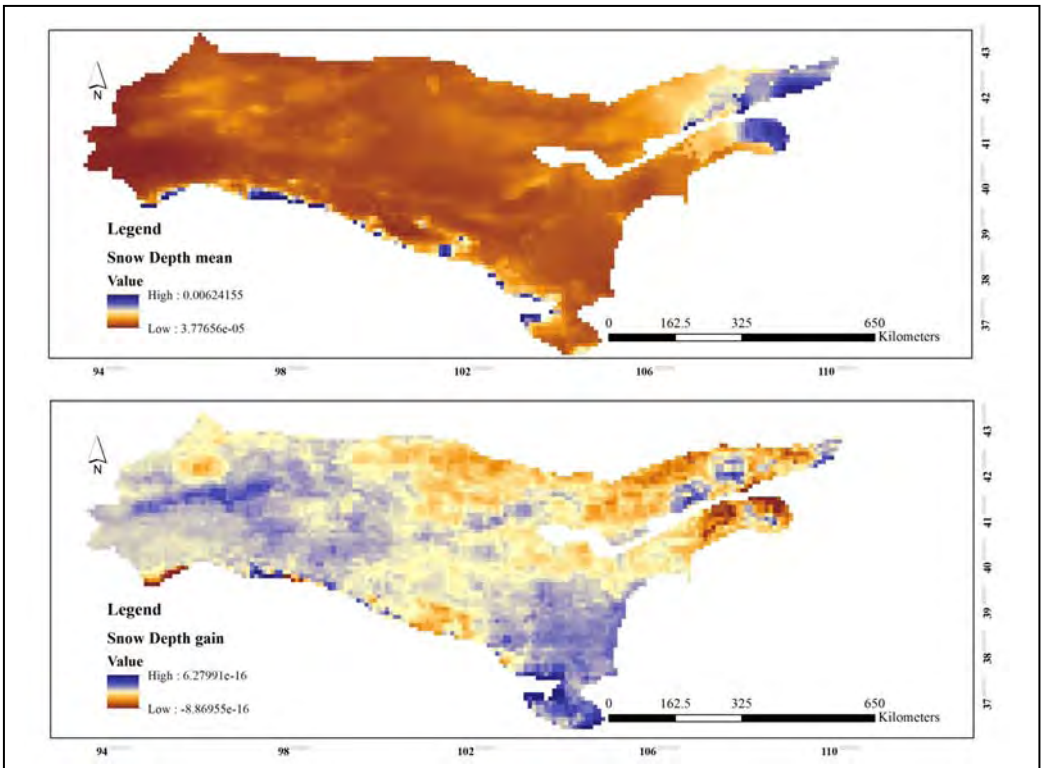
N
Legend
Snow Depth mean
Value
High : 0.00624155
Low : 3.77656e-05
0 162.5 325 650
Kilometers
94 98 102 106 110
37 38 39 40 41 42 43
N
Legend
Snow Depth gain
Value
High : 6.27991e-16
Low : -8.86955e-16
0 162.5 325 650
Kilometers
94 98 102 106 110
37 38 39 40 41 42 43

(k)

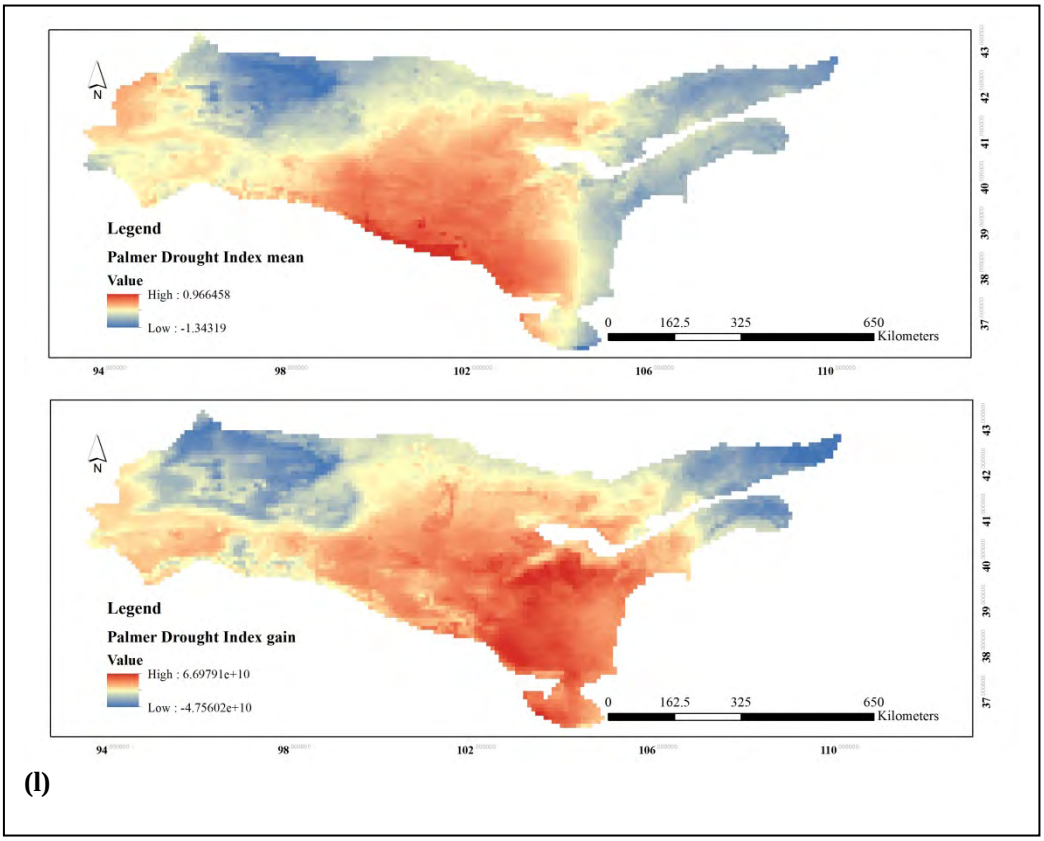
N
Legend
Palmer Drought Index mean
Value
High : 0.966458
Low : -1.34319
0 162.5 325 650
Kilometers
94 98 102 106 110
37 38 39 40 41 42 43
N
Legend
Palmer Drought Index gain
Value
High : 6.69791e+10
Low : -4.75602e+10
0 162.5 325 650
Kilometers
94 98 102 106 110
37 38 39 40 41 42 43

(l)

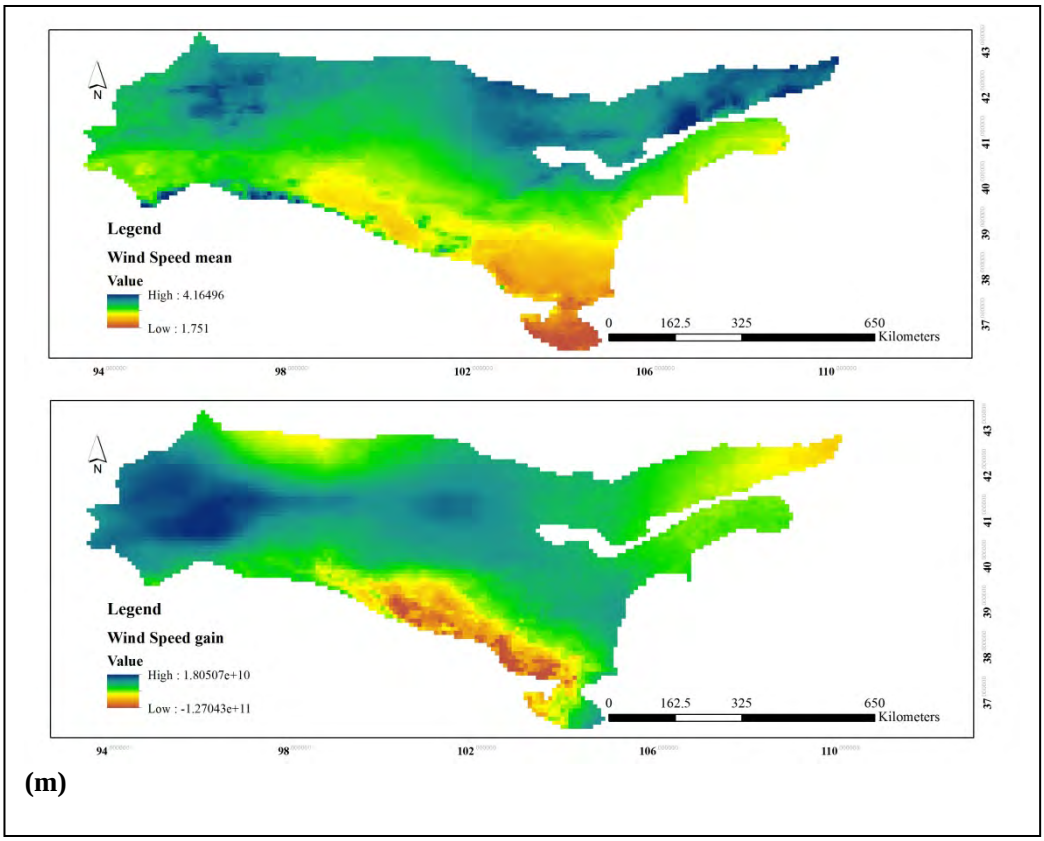

Fig. 5 Patterns of the climate and environment drivers such as Air Temperature (a), Total Precipitation (b), Surface Pressure (c), Soil Heat Flux (d), Sensible Heat Flux (e), Latent Heat Flux (f), Soil Moisture (g), Downward Longwave Radiation (h), Downward Shortwave Radiation (i), Snow Water Equivalent (j), Snow Depth (k), The Palmer Drought Severity Index (l), Wind Speed (m) in the Alashan Plateau semi-desert.

4 Conclusions

In this study, we examined the response of vegetation indicators to climate parameters affecting climate change in the Alashan Plateau semi-desert from 1982 to 2019. The results effectively showed the effects of climate change on vegetation dynamics. Overall, we found that the current trend of changes in the parameters affecting climate change, such as rising temperatures, transpiration-evaporation, soil temperature, solar radiation, and reduction in rain and snow in the Alashan Plateau Semi-Desert, reduces vegetation indicators. In other words, the phenomenon of browning due to climate change occurs, and three forest cover indices, LAI, FAPAR, and NDVI, decreased by about 6-10, 6-7, and 19-20 % correspondingly. In general, it can be said that climate change in hot and dry regions and highlands such asAlashan Plateau Semi-Desert has adverse effects. With the current climate change trends, such as increasing temperature and decreasing rainfall, reducing the dynamics of vegetation indices in these areas can be seen dramatically. In addition to climatic factors, the impact of human activities on the process of vegetation change can also be mentioned because humans can increase the harmful effects of climate change by destroying forests, pastures, and green spaces and increasing urban development. These changes can have many consequences, including soil erosion, biodiversity loss, flood intensification, and global warming.

On the other hand, increasing afforestation, conservation of natural resources, land use management, and implementation of projects such as carbon zero and the Kyoto Protocol can help in stabilizing the climate and

reducing severe weather events and positive results from climate stabilization such as reducing the global temperature, reduce drought, reduce flood risk, etc. Therefore, it can be said that to protect the environment better and reduce the severe effects of climate change, we must pay more attention to climate change on vegetation in the context of global warming. As well as reducing the negative effects of climate change by taking preventive actions such as land use management, afforestation, and vegetation conservation.

Acknowledgement

All rights reserved. Thank you to all those who collaborated on this paper.

References

Baret F, Guyot G, Major DJ. 1989. Crop biomass evaluation using radiometric measurements. Photogrammetria, 43(5): 241-256

Berry J. 2018. 3.10 solar induced chlorophyll fluorescence: Origins, relation to photosynthesis and retrieval. Comprehensive Remote Sensing, 3: 143-162

Braswell, B. H, Schimel, D. S, Linder, E, Moore Iii, B. 1997. The response of global terrestrial ecosystems to interannual temperature variability. Science, 278(5339): 870-873

Chen H, Shao L, Zhao M, Zhang X, Zhang D. 2017. Grassland conservation programs, vegetation rehabilitation and spatial dependency in Inner Mongolia, China. Land Use Policy, 64: 429-439

Chen T, Bao A, Jiapaer G, Guo H, Zheng G, Jiang L, et al. 2019. Disentangling the relative impacts of climate change and human activities on arid and semiarid grasslands in Central Asia during 1982–2015. Science of the Total Environment, 653: 1311-1325

Chu H, Venevsky S, Wu C, Wang M. 2019. NDVI-based vegetation dynamics and its response to climate changes at Amur-Heilongjiang River Basin from 1982 to 2015. Science of the Total Environment, 650: 2051-2062

Cleland EE, Chuine I, Menzel A, Mooney HA, Schwartz MD. 2007. Shifting plant phenology in response to global change. Trends in Ecology and Evolution, 22(7): 357-365

De Beurs KM, Henebry GM, Owsley, BC, Sokolik I. 2015. Using multiple remote sensing perspectives to identify and attribute land surface dynamics in Central Asia 2001–2013. Remote Sensing of Environment, 170: 48-61

De Jong R, de Bruin S, de Wit A, Schaepman ME, Dent DL. 2011. Analysis of monotonic greening and browning trends from global NDVI time-series. Remote Sensing of Environment, 115(2): 692-702

Deng C, Zhang B, Cheng L, Hu L, Chen F. 2019. Vegetation dynamics and their effects on surface water-energy balance over the Three-North Region of China. Agricultural and Forest Meteorology, 275: 79-90

Deng H, Chen Y. 2017. Influences of recent climate change and human activities on water storage variations in Central Asia. Journal of Hydrology, 544: 46-57

Fahad S, Sonmez O, Saud S, Wang D, Wu C, Adnan M, Turan V. 2021. Climate Change And Plants: Biodiversity, Growth and Interactions. CRC Press, USA

Fahad S, Sonmez O, Saud S, Wang D, Wu C, Adnan M, Turan V. 2021. Plant Growth Regulators for Climate-Smart Agriculture. CRC Press, USA

Fahad S, Sonmez O, Saud S, Wang D, Wu, C, Adnan M, Turan V. 2021. Developing Climate-Resilient Crops: Improving Global Food Security And Safety. CRC Press, USA

Gao W, Zheng C, Liu X, Lu Y, Chen Y, Wei Y, Ma Y. 2022. NDVI-based vegetation dynamics and their responses to climate change and human activities from 1982 to 2020: A case study in the Mu Us Sandy Land, China. Ecological Indicators, 137: 108745

Gao X, Huang X, Lo K, Dang Q, Wen R. 2021. Vegetation responses to climate change in the Qilian Mountain Nature Reserve, Northwest China. Global Ecology and Conservation, 28: e01698

Guo E, Wang, Y, Wang C, Sun Z, Bao Y, Mandula N, et al. 2021. NDVI indicates long-term dynamics of vegetation and its driving forces from climatic and anthropogenic factors in Mongolian Plateau. Remote Sensing, 13(4): 688

Huang MT, Zhou BQ, Zha PM. 2020. Impacts of extreme weather and climate events on desertification, land degradation and food security. Advances in Climate Change Research, 16(1): 17

Jeong SJ, Ho, CH, Gim HJ, Brown ME. 2011. Phenology shifts at start vs. end of growing season in temperate vegetation over the Northern Hemisphere for the period 1982–2008. Global Change Biology, 17(7): 2385-2399

Jeong S, Park H. 2021. Toward a comprehensive understanding of global vegetation CO2 assimilation from space. Global Change Biology, 27(6): 1141-1143

Jiang L, Liu Y, Wu S, Yang C. 2021. Analyzing ecological environment change and associated driving factors in China based on NDVI time series data. Ecological indicators, 129: 107933

Kong D, Miao C, Duan Q, Lei X, Li H. 2018. Vegetation‐Climate Interactions on the Loess Plateau: A Nonlinear Granger Causality Analysis. Journal of Geophysical Research: Atmospheres, 123(19): 11-068.

Kong D, Miao C, Wu J, Zheng H, Wu S. 2020. Time lag of vegetation growth on the Loess Plateau in response to climate factors: Estimation, distribution, and influence. Science of The Total Environment, 744: 140726

Li P, Wang J, Liu M, Xue Z, Bagherzadeh A, Liu M. 2021. Spatio-temporal variation characteristics of NDVI and its response to climate on the Loess Plateau from 1985 to 2015. Catena, 203: 105331

Li X, Jiang L, Meng F, Wang S, Niu H, Iler AM, et al. 2016. Responses of sequential and hierarchical phenological events to warming and cooling in alpine meadows. Nature Communications, 7(1): 12489

Linderholm HW. 2006. Growing season changes in the last century. Agricultural and Forest Meteorology, 137(1-2): 1-14

Liu C, Li W, Wang W, Zhou H, Liang T, Hou F, et al. 2021. Quantitative spatial analysis of vegetation dynamics and potential driving factors in a typical alpine region on the northeastern Tibetan Plateau using the Google Earth Engine. Catena, 206: 105500

Liu Q, Liu L, Zhang Y, Wang Z, Wu J, Li L, et al. 2021. Identification of impact factors for differentiated patterns of NDVI change in the headwater source region of Brahmaputra and Indus, Southwestern Tibetan Plateau. Ecological Indicators, 125: 107604

Liu Y, Lei H. 2015. Responses of natural vegetation dynamics to climate drivers in China from 1982 to 2011. Remote Sensing, 7(8): 10243-10268

Lotsch A, Friedl MA, Anderson BT, Tucker CJ. 2005. Response of terrestrial ecosystems to recent Northern Hemispheric drought. Geophysical Research Letters, 32(6)

Nord EA, Lynch JP. 2009. Plant phenology: a critical controller of soil resource acquisition. Journal of experimental botany, 60(7): 1927-1937

Ols C, Kålås IH, Drobyshev I, Söderström L, Hofgaard A. 2019. Spatiotemporal variation in the relationship between boreal forest productivity proxies and climate data. Dendrochronologia, 58: 125648

Parmesan C, Yohe G. 2003. A globally coherent fingerprint of climate change impacts across natural

systems. Nature, 421(6918): 37-42

Peñuelas J, Filella I, Zhang X, Llorens L, Ogaya R, Lloret F, et al. 2004. Complex spatiotemporal phenological shifts as a response to rainfall changes. New Phytologist, 161(3): 837-846

Piao S, Liu Q, Chen A, Janssens IA, Fu Y, Dai J, et al. . 2019. Plant phenology and global climate change: Current progresses and challenges. Global Change Biology, 25(6): 1922-1940

Piao S, Wang X, Wang K, Li X, Bastos A, Canadell JG, et al. 2020. Interannual variation of terrestrial carbon cycle: Issues and perspectives. Global Change Biology, 26(1): 300-318

Prăvălie R. 2018. Major perturbations in the Earth's forest ecosystems. Possible implications for global warming. Earth-Science Reviews, 185: 544-571

Ramos MC. 2017. Projection of phenology response to climate change in rainfed vineyards in north-east Spain. Agricultural and forest meteorology, 247: 104-115

Shang J, Zhang Y, Peng Y, Huang Y, Zhu L, Wu Z, et al. 2022. Climate change drives NDVI variations at multiple spatiotemporal levels rather than human disturbance in Northwest China. Environmental Science and Pollution Research, 1-15

Shen Y, Liu, X. 2015. Phenological changes of corn and soybeans over US by Bayesian change-point model. Sustainability, 7(6): 6781-6803

Shi S, Yu J, Wang F, Wang P, Zhang Y, Jin K. 2021. Quantitative contributions of climate change and human activities to vegetation changes over multiple time scales on the Loess Plateau. Science of the Total Environment, 755: 142419

Shuting LI, et al. 2019. Spatial-temporal variation of NDVI and its responses to precipitation and temperature in Inner Mongolia from 2001 to 2015. Journal of University of Chinese Academy of Sciences, 36(1): 48

Song Y, Wang J, Yu Q, Huang J. 2020. Using MODIS LAI data to monitor spatio-temporal changes of winter wheat phenology in response to climate warming. Remote Sensing, 12(5): 786

Sun R, Chen S, Su H. 2021. Climate dynamics of the spatiotemporal changes of vegetation NDVI in northern China from 1982 to 2015. Remote Sensing, 13(2): 187

Sun Y, Yang Y, Zhang L, Wang Z. 2015. The relative roles of climate variations and human activities in vegetation change in North China. Physics and Chemistry of the Earth, Parts A/B/C, 87: 67-78

Tao Z, Wang H, Liu Y, Xu Y, Dai J. 2017. Phenological response of different vegetation types to temperature and precipitation variations in northern China during 1982–2012. International Journal of Remote Sensing, 38(11): 3236-3252

Verger A, Filella I, Baret F, Peñuelas J. 2016. Vegetation baseline phenology from kilometric global LAI satellite products. Remote Sensing of Environment, 178: 1-14

Visser ME, Both C. 2005. Shifts in phenology due to global climate change: the need for a yardstick. Proceedings of the Royal Society B: Biological Sciences, 272(1581): 2561-2569

Wang F, Chen B, Lin X, Zhang H. 2020. Solar-induced chlorophyll fluorescence as an indicator for determining the end date of the vegetation growing season. Ecological Indicators, 109: 105755

Wang H, Li Z, Cao L, Feng R, Pan Y. 2021. Response of NDVI of natural vegetation to climate changes and drought in China. Land, 10(9): 966

Wang S, Yang B, Yang Q, Lu L, Wang X, Peng Y. 2016. Temporal trends and spatial variability of vegetation phenology over the Northern Hemisphere during 1982-2012. PloS one, 11(6): e0157134

Xie Y, Wang X, Silander Jr JA. 2015. Deciduous forest responses to temperature, precipitation, and drought imply complex climate change impacts. Proceedings of the National Academy of Sciences, 112(44): 13585-13590

Xiong J, Ye C, Cheng W, Guo L, Zhou C, Zhang X. 2019. The spatiotemporal distribution of flash floods and analysis of partition driving forces in Yunnan Province. Sustainability, 11(10): 2926

Zhao Y, Chi W, Kuang W, Bao Y, Ding G. 2020. Ecological and environmental consequences of ecological projects in the Beijing–Tianjin sand source region. Ecological Indicators, 112: 106111

Zhe M, Zhang X. 2021. Time-lag effects of NDVI responses to climate change in the YamzhogYumco Basin, South Tibet. Ecological Indicators, 124: 107431

Zhou L, Zhou W, Chen J, Xu X, Wang Y, Zhuang J, Chi Y. 2022. Land surface phenology detections from multi-source remote sensing indices capturing canopy photosynthesis phenology across major land cover types in the Northern Hemisphere. Ecological Indicators, 135: 108579

Zhu L, Meng J, Zhu L. 2020. Applying Geodetector to disentangle the contributions of natural and anthropogenic factors to NDVI variations in the middle reaches of the Heihe River Basin. Ecological Indicators, 117: 106545

Zhu W, Jiang N, Chen G, Zhang D, Zheng Z, Fan D. 2017. Divergent shifts and responses of plant autumn phenology to climate change on the Qinghai-Tibetan Plateau. Agricultural and Forest Meteorology, 239: 166-175